



TECHNISCHE  
UNIVERSITÄT  
WIEN

Project Report

# Preliminary research on an electron beam setup for the QUAK experiment

performed at Atominstitut



at Technische Universität Wien  
Faculty of Physics

under the supervision of  
**Assistant Prof. Dr.rer.nat. Philipp Haslinger**  
and  
**Projektass.(FWF) Dipl.-Ing. Thomas Weigner**

by \_\_\_\_\_

set date to Eng

**Frank Takara Ebel & Alexander Preimesberger**

Matrikelnummer: 01429282 & 01427641

Stadionallee 2  
1020 Wien

Wien, am 15-05-2020

# Contents

<b>1 Short introduction to QUAK</b>	<b>1</b>
<b>2 Cathodic Ray Tube Basics</b>	<b>2</b>
2.1 Underlying Physics . . . . .	2
2.2 Implementation in the Heerlen D14-363GY . . . . .	5
2.2.1 The Cathode . . . . .	7
2.2.2 Cathode Layout . . . . .	8
<b>3 Cicero Word Generator</b>	<b>10</b>
3.1 Installation of National Instruments drivers . . . . .	10
3.2 Installation of National Instruments Cards . . . . .	10
3.3 Configuring Atticus . . . . .	10
3.3.1 Configure hardware timing / synchronization . . . . .	11
3.4 Configuration and Basic Usage of Cicero . . . . .	12
3.5 Saving of Settings and Sequences . . . . .	12
3.6 Sequence length limit . . . . .	12
<b>4 Electron beam setup</b>	<b>13</b>
4.1 Charatarization of a working CRT . . . . .	13
4.2 High Voltage Power Supply HVPS . . . . .	14
4.2.1 Ripple measurement . . . . .	15
4.3 CRT wiring . . . . .	16
4.4 Heater . . . . .	17
<b>5 CRT handling</b>	<b>19</b>
5.1 Opening CRTs . . . . .	19
5.1.1 Rotary tool . . . . .	19
5.1.2 Wire cutting . . . . .	19
5.2 Oxygen poisoning . . . . .	20
<b>6 Vacuum test chamber</b>	<b>23</b>
6.1 First iteration . . . . .	23
6.1.1 Parts . . . . .	23
6.1.2 CRT mounting mechanism . . . . .	24
6.1.3 Leak test . . . . .	25
6.2 Second iteration . . . . .	25
6.2.1 Changes . . . . .	25

6.2.2	Fastening	26
<b>7</b>	<b>Deflection Electronics</b>	<b>27</b>
7.1	Demands on the setup	27
7.2	Implementation	28
<b>8</b>	<b>Beam Characterization</b>	<b>32</b>
8.1	Aluminum foil	32
8.2	Faraday cup	33
8.3	Deflection frequency	34
<b>9</b>	<b>Next Steps</b>	<b>36</b>
	<b>Todo list</b>	<b>37</b>
	<b>References</b>	<b>39</b>

# <sup>1</sup> 1 Short introduction to QUAK

<sup>2</sup> The goal of QUAK (quantum klystron) is to drive Rabi oscillations between hyperfine  
<sup>3</sup> levels of  $^{39}\text{K}$  which has a frequency of 461.7 MHz [1] using a classical electron beam.  
<sup>4</sup> For this, it is necessary to Doppler cool the atoms in a MOT (magneto-optical trap)  
<sup>5</sup> using lasers. Once the atoms are trapped, they will be exposed to the near-field of the  
<sup>6</sup> electron beam, which will be spatially modulated with the transition frequency. In  
<sup>7</sup> order to achieve this goal, the beam must allow for a current of 100  $\mu\text{A}$  and a beam  
<sup>8</sup> waist of 100  $\mu\text{m}$ .

<sup>9</sup> In our work, we conducted first experiments on how to accomplish an electron beam  
<sup>10</sup> fulfilling those requirements.

# 2 Cathodic Ray Tube Basics

This section features a quick explanation what a CRT is and what its main components are, followed by a more detailed description on how these components are implemented in the CRT Heerlen D14-363GY, which was used in this project. It ends with a description of the important characteristics of the CRT and the requirement the theory poses on them.

## 2.1 Underlying Physics

Wikipedia states: “The cathode-ray tube (CRT) is a vacuum tube that contains one or more electron guns and a phosphorescent screen and is used to display images. It modulates, accelerates, and deflects electron beam(s) onto the screen to create the images.”

There are three vital components to accomplish this feat: the electron gun, the electron lens and the deflection plates.

The electron gun extracts electrons from a cathode material, accelerates them onto a perforated anode and thereby produces a free electron beam (see fig. 2.1). One important characteristic in the selection of a cathode material is a low work function. It denotes the amount of energy needed to extract one electron from the material. There are two ways to overcome this energy barrier in an electron gun; one can either overcompensate it by applying a strong electric field (“field emission”, “cold cathode”, fig. 2.2b); or one can heat the material until some electrons have enough thermal energy to overcome the energy barrier (“thermal emission”, “hot cathode”, fig. 2.2a). For our CRT, only thermal emission is relevant, more detail on this will be added later along with the description of our cathode’s design.

The cathode itself is housed in a so-called Wehnelt cylinder, as the name suggests it is conducting cylinder which is set to a slightly more negative potential than the cathode itself. This part implements two features; firstly it condenses the emitted electrons, leading to a smaller spot size, i.e. making the cathode a more point-like electron source. Secondly it enables us to regulate the beam current, the more negative the Wehnelt potential is, the less electrons are emitted by the electron gun. As we

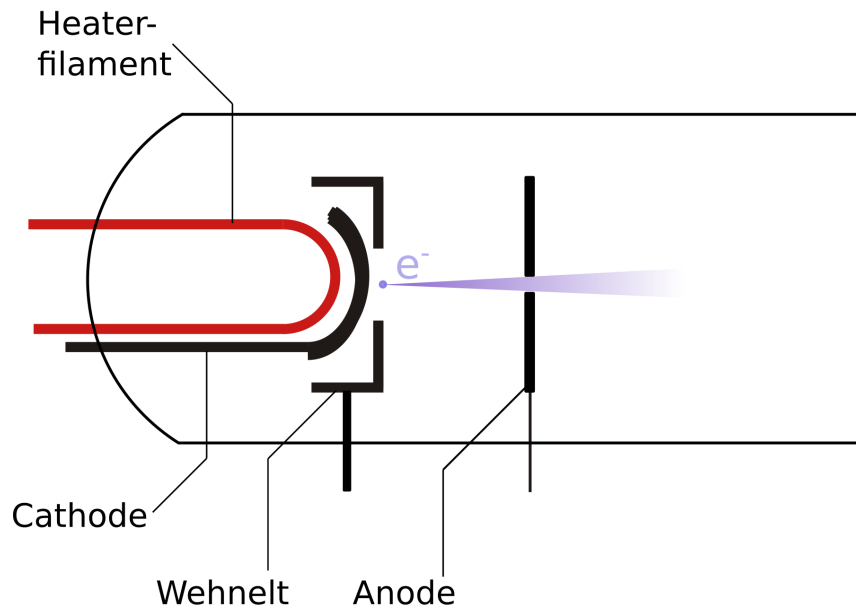
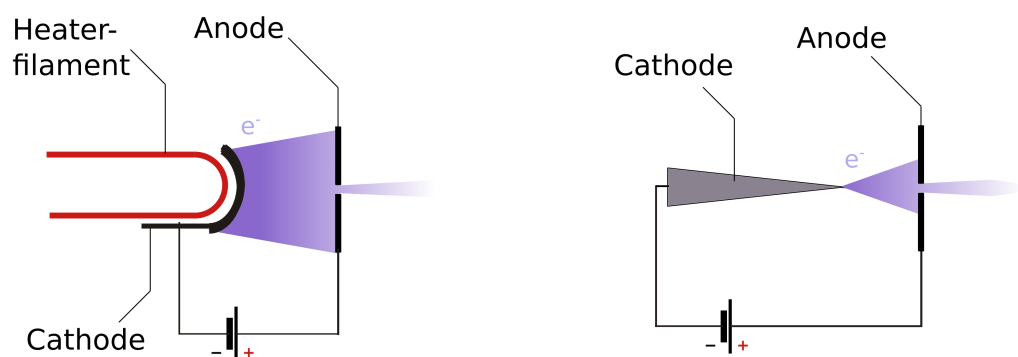


**Figure 2.1:** Schematic of an electron gun



(a) Schematic of a hot cathode

(b) Schematic of field emission cathode

**Figure 2.2:** Cathode types

make the Wehnelt potential more positive, the beam current increases and continues to rise even after it is more positive than the cathode itself. However the spot size reduction is lost in the process, along with the ability to properly focus the beam with electron optics.

The electrons that leave the electron gun are still divergent and need to be focused. For our 2 keV electrons it is still possible to use an electrostatic lens. Cylindrically symmetrical pieces of conductor, like rings and tubes, can be set to an electrical potential and act as a lens for the electrons. By combining several of them, one can (theoretically) engineer an electro-optical system with any combination of desired focal lengths  $f_1$  and  $f_2$ . The field of this system is simply governed by Laplace's equation in cylindrical coordinates:

$$0 = \frac{1}{r} \frac{\partial \phi}{\partial r} + \frac{\partial^2 \phi}{\partial r^2} + \frac{\partial^2 \phi}{\partial z^2} \quad (2.1)$$

If we take the axis of the beam to be the z-axis, the focal point position in the x-y-plane can be shifted using the two pairs of deflection plates, one for the x- and one for the y-direction. The deflection is achieved by applying a voltage between the two parallel plates. (see: fig. 2.3) By starting with an electron with kinetic energy  $e \cdot U_0$  which is accelerated in x-direction by a constant force  $e \cdot U_x/d$  over the extent of the plates  $L$ , the deflection angle is approximately [2]:

$$\delta \approx \tan(\delta) \approx \frac{U_x \cdot L}{2U_0 \cdot d} \quad (2.2)$$

For the measures of our CRT ( $L \approx 10$  cm,  $d \approx 1$  cm,  $U_0 \approx 2$  kV and distance to screen  $\approx 20$  cm) this amounts to a deflection coefficient of around  $20$  V cm $^{-1}$ , which is quite consistent with the value given in the CRT's manual.

2 können die Ma  
stimmen?

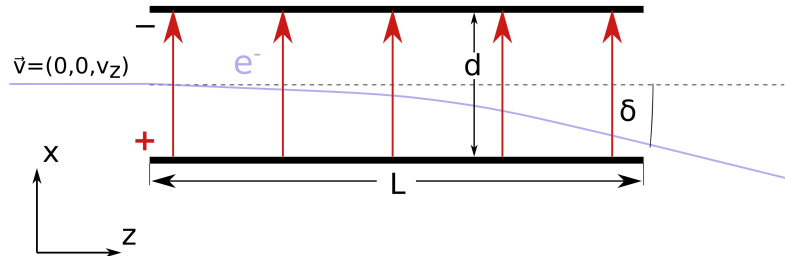


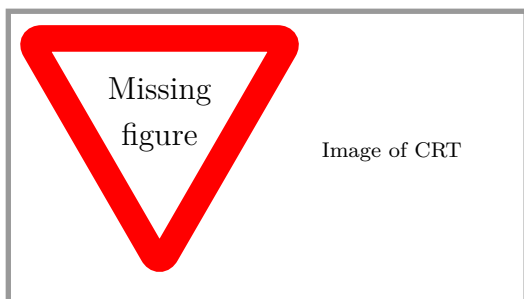
**Figure 2.3:** Deflection of an electron beam in a constant electrical field

## **2.2 Implementation in the Heerlen D14-363GY**

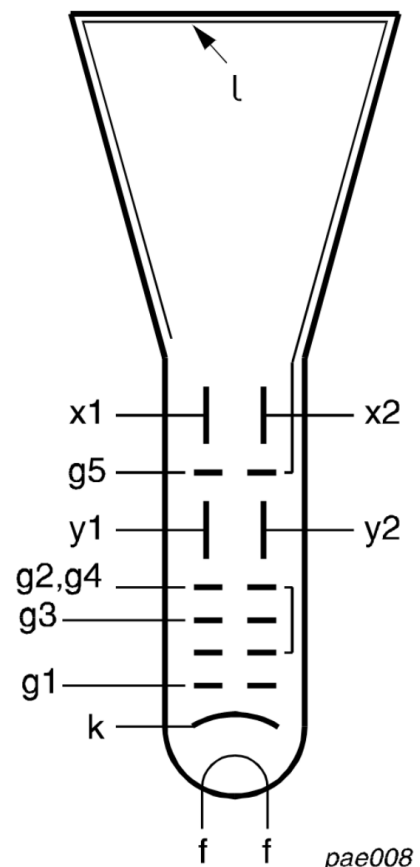
This section describes how the mechanisms described above are implemented in the CRT that was used in this project: the PDS/CRT Heerlen D14-363GY. Figure 2.4a shows an image of said CRT, fig. 2.4b shows a schematic depiction. The cathode is not visible, as it is fixed inside the Wehnelt cylinder (1), just a few millimeters from the exit of the wehnelt cylinder the electrons pass through the perforated anode (2) they gain their full final kinetic energy over this short distance. The electrons that go through the perforation and enter the electrostatic lens, have 2 keV and therefore move at a speed of approximately  $0.08 c$ . The electrostatic lenses are realized using three conducting rings (3), that are set to the same potential but have varying radii: Each consecutive ring has a smaller radius than the previous one.

Between the electrostatic lens and the deflection plates, there is another aperture (4), which is internally connected to the anode and is thereby kept at the same potential. In our Setup, the deflection plates are not simply parallel but are shaped like funnels (5,7), between the two pairs of deflection plates, we have the final aperture (6), this ones potential can be regulated separately (usually it's on the same potential as the anode)

It is connected to the aquadag coating inside the glass envelope and prevents charge up and image distortion. Finally the beam hits the phosphorous-coated screen which fluoresces on electron impact.



(a) Image picture of the Heerlen D14-363GY



(b) Schematic of the CRT from [3]

**Figure 2.4**

### <sup>1</sup> 2.2.1 The Cathode

<sup>2</sup> As already mentioned, we are using a hot cathode, where electrons are excited thermally  
<sup>3</sup> until some of them acquire enough energy to leave the material. Compared to cold  
<sup>4</sup> cathodes which work by field emission, this leads to a broader energy distribution. In  
<sup>5</sup> fields like electron microscopy, where a high resolution is the goal, this is undesirable as  
<sup>6</sup> it leads to some degree of chromatic aberration in the electron optics; for our purposes,  
<sup>7</sup> this should not be a problem. On the other hand, hot cathodes normally allow for  
<sup>8</sup> higher current densities, which is very important to us. The electron current from this  
<sup>9</sup> kind of emission is described by [4, chp 3.2.3]:

<sup>10</sup> 
$$I = A \cdot T^2 \cdot e^{-b/T} \quad (2.3)$$

<sup>11</sup> Where  $b$  is proportional to the work function of the material,  $T$  is temperature and  
<sup>12</sup>  $A$  is a material-dependent constant. It is clear from this formula, that a low work  
<sup>13</sup> function and a high melting point are important characteristics for a good cathode  
<sup>14</sup> material.

<sup>15</sup> The cathode from one of our Heerlen D14-363GY-tubes has been removed and  
<sup>16</sup> examined with EDX (Energy-dispersive X-ray Spectroscopy). Nickel, barium, and  
<sup>17</sup> strontium have been found, which suggests that it is a metal oxide cathode with barium-,  
<sup>18</sup> strontium-, and possibly aluminum-oxide. This type of cathode is very common in low  
<sup>19</sup> power electron tubes.

<sup>20</sup> The “Power Vacuum Tubes Handbook” [4, chp 3.5.2.1] describes a typical oxide  
<sup>21</sup> cathode as a coating of barium and strontium oxides on a structure made from nickel  
<sup>22</sup> alloys. Nickel is chosen for its strength and toughness, which it retains even at  
<sup>23</sup> high temperatures. These cathodes are normally made by coating a case structure  
<sup>24</sup> with a mixture of barium and strontium carbonates (typically 60 % Ba and 40 % Sr),  
<sup>25</sup> suspended in a binder material and then baking the structure, causing the carbonates  
<sup>26</sup> to be reduced to oxides.

<sup>27</sup> These metal oxide cathodes normally operate at 700 °C to 820 °C and are capable of  
<sup>28</sup> average emission densities of 100 mA cm<sup>-2</sup> to 500 mA cm<sup>-2</sup>. Still higher peak emissions  
<sup>29</sup> are possible for shorter periods of time; as already mentioned, one of the advantages of  
<sup>30</sup> this type of cathode is its high emission current capability compared to cathodes made  
<sup>31</sup> from other materials. Downsides to this cathode type are its greater susceptibility  
<sup>32</sup> to so-called oxygen poisoning and to ion bombardment. The literature therefore  
<sup>33</sup> recommends to avoid prolonged exposure to oxygen. Oxygen poisoning is the process  
<sup>34</sup> in which oxygen adsorbs onto the cathode and increases its work function, effectively  
<sup>35</sup> reducing the ability to emit electrons. Also the material from the oxide cathode will

evaporate during the tube's lifetime and will travel to other parts of the tube, adsorbing to electron optics parts and turning them into additional emitters. The literature (also from [4, chp 3.5.2.1]) therefore also advises against exceeding the design value for the heater voltage, as this reduces the lifetime of the cathode significantly. (However during the course of our project, we did drive the cathode with higher heater voltages on various occasions in order to increase the available beam current.)

## 2.2.2 Cathode Layout

Figure 2.5 shows how metal oxide cathodes for CRTs typically look; the depiction agrees very well with the layout of our cathode. On the image we see the cathode cylinder, which corresponds to the nickel support structure mentioned above. It is shaped into a cup, i.e. the cylinder is hollow and open on one side, where the heater filament (shaped into a heater coil) is inserted. The oxide disk, from where the electrons are emitted, is baked onto the top of the cathode cylinder. The cathode cylinder is mounted on an isolating support structure and inserted into the Wehnelt cylinder, which is called "grid cup" in the drawing.

## 2 Cathodic Ray Tube Basics

---

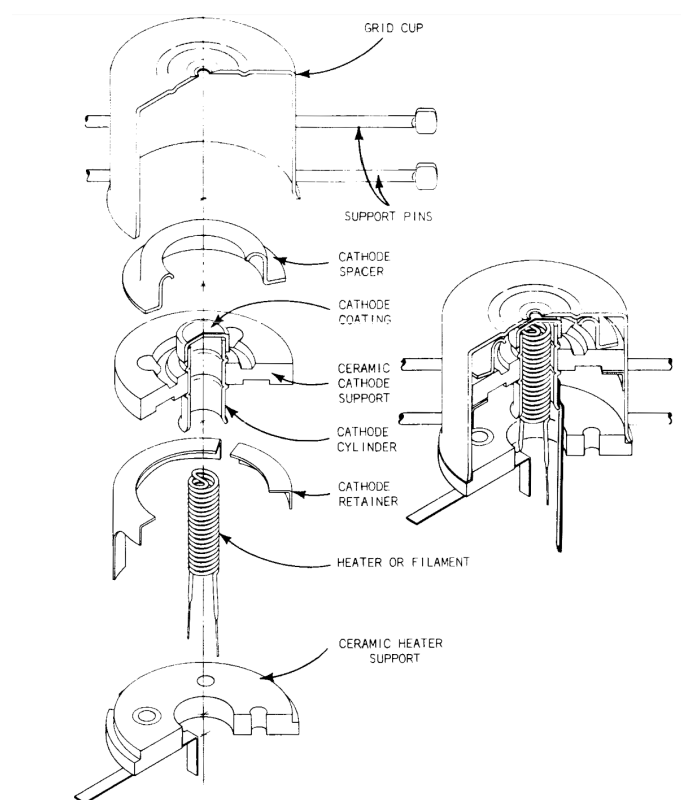


**Figure 2.5:** Schematic of the layout of a typical CRT-cathode from [5]

# 3 Cicero Word Generator

This chapter describes the installation and initial setup of Cicero Word Generator [6] on a PC running Windows 10 with analog and digital cards from National Instruments (NI). The code is freely available on GitHub [7]. This chapter contains only differences, problems, and possible solutions encountered when Cicero was installed for the PC ‘Fritz Fantom’ which will be used for the QuaK experiment. It is therefore advised to use the technical and user manual [8] in conjunction. The titles in this chapter and font style with **Courier** and **Boldface** was mirrored in order to fit the manual.

## 3.1 Installation of National Instruments drivers

Before setting up the Cicero Word Generator, it is necessary to install the newest .NET Framework [9] from Microsoft. For the first installation of NI drivers, NI-DAQmx (version 9.3), NI-VISA (newest version), and NI-4888.2 (newest version) should be downloaded from the National Instruments website [10]. When installing the NI drivers it is possible to get an ‘Runtime Error!’. In this case it is necessary to set the Regional format settings of Windows 10 to ‘English (United States)’ [11].

## 3.2 Installation of National Instruments Cards

After installation of the necessary drivers, the physical cards can be inserted into the PCIe slots on the motherboard. On ‘Fritz Fantom’ the digital card (NI PCIe-6537B) was installed in PCIe bus 3 while the analog cards (NI PCIe-6738) were installed in PCIe bus 4 and 5.

## 3.3 Configuring Atticus

After installation of the NI cards, Atticus should be launched for the first time and closed without changing any settings. After this, the NI-DAQmx drivers should be

1 updated to the newest version. If version 9.3 was not used when launching Atticus  
2 in this step, it could result in an error. After this, “Configuring Atticus” on the  
3 user manual can be followed. The **Server Name** was set to ‘Fritz\_Phantom’. **Dev1**  
4 to **Dev3** were set in the same ascending order as the physical installation on the  
5 motherboard.

change server name  
in lab? Fantom  
Phantom

### 6 3.3.1 Configure hardware timing / synchronization

7 For synchronization, a **Shared Sample Clock** was used with **Dev1** being the master  
8 card. The settings are summarized in table 3.1 and table 3.2. **Dev3** follows the same  
9 settings as **Dev2** except ‘SampleClockExternalSource’ was set to ‘/Dev3/RTSI7’. The  
10 ‘SampleClockRate’ is set to 350 kHz since this is the fastest rate with all 32 analog  
11 channels active. It is possible to raise this to 1 MHz by only using 8 channels (1 channel  
12 per bank).

**Table 3.1:** Settings for **Dev1**.

Setting	Value
MasterTimebaseSource	
MySampleClockSource	DerivedFromMaster
SampleClockRate	350000
UsingVariablenamebase	False
SoftTriggerLast	True
StartTriggerType	SoftwareTrigger

**Table 3.2:** Settings for **Dev2**.

Setting	Value
MasterTimebaseSource	
MySampleClockSource	External
SampleClockExternalSource	/Dev2/RTSI7
SampleClockRate	350000
UsingVariablenamebase	False
SoftTriggerLast	False
StartTriggerType	SoftwareTrigger

## 3.4 Configuration and Basic Usage of Cicero

After setting up the Atticus server, Cicero can be configured. In step 3.c. it is necessary  
to write the full IP address and not ‘localhost’. Once step 6 is finished, Cicero should  
run without any problems.

## 3.5 Saving of Settings and Sequences

The ‘SettingsData’ of the Server Atticus are saved in C:\Users\confetti\Documents  
\Cicero\_Atticus\Cicero\SettingsData while the ‘SequenceData’ of Cicero are saved in  
C:\Users\confetti\Documents\Cicero\_Atticus\Cicero\SequenceData.

## 3.6 Sequence length limit

The duration of a sequence is limited to  $2^{32}/(16 * 32 * 350 \text{ kHz}) = 23.967 \text{ s}$  coming  
from a 32-bit application, 16 bit per channel, 32 channels in a NI PCIe-6738 card, and  
350 kHz clock rate.

# <sup>1</sup> 4 Electron beam setup

## <sup>2</sup> 4.1 Charatarization of a working CRT

<sup>3</sup> HAMEG HM507 oscilloscopes [12] were used for testing purposes which contain a  
<sup>4</sup> D14-363GY/123[3] CRT. Although it only has a bandwidth of 0MHz to 50MHz,  
<sup>5</sup> which is not sufficient for the hyperfine splitting frequency of 461.7MHz of <sup>39</sup>K, it was  
<sup>6</sup> used nevertheless because of its simple construction and availability. The back pin  
<sup>7</sup> arrangement is shown in fig. 4.1.

<sup>8</sup> The voltages and currents of the necessary pins to drive the CRT were measured  
<sup>9</sup> using a 2.5kV probe with an attenuation ratio of and are summarized in table 4.1. It  
<sup>10</sup> was not possible to measure pin g3 directly. Therefore a HVPS (section 4.2) was used  
<sup>11</sup> to set a voltage and the beam diameter was observed. The best focus was achieved  
<sup>12</sup> with the value written in the table. The voltage offset of x-, and y-plates was not  
<sup>13</sup> possible to measure directly, since it varies with time to draw the necessary image on  
<sup>14</sup> the phosphor screen. The given values are the mean of the minimum and maximum  
<sup>15</sup> measured voltage. The deflection coefficient is summarized in table 4.2.

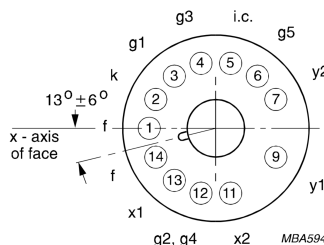


**Figure 4.1:** Pin arrangement, bottom view from [3]

**Table 4.1:** D14-363GY/123 CRT pin measurements

number	pin	voltage/V	current/ $\mu\text{A}$
1	f	$-1.99 \times 10^3$	$86.6 \times 10^3$
2	k	$-2.00 \times 10^3$	-7.6
3	g1	$-2.03 \times 10^3$	0
4	g3	$-1.813 \times 10^3$	0
5	i.c.	71.7	0.1
6	g5	64.0	7.2
7	y2	78	-
9	y1	78	-
11	x2	96	-
12	g2, g4	71.0	0
13	x1	96	-
14	f	$-1.97 \times 10^3$	$-86.2 \times 10^3$

**Table 4.2:** D14-363GY/123 deflection coefficient from [3]

horizontal	$M_x$	19 V/cm
vertical	$M_y$	11.5 V/cm

## 4.2 High Voltage Power Supply HVPS

To produce high dc voltages to drive the CRT, four HCP 14-6500 power supplies [13] were used. They were named ‘HVPS 1’ to ‘HVPS 4’ and can provide up to  $\pm 6.5$  kV and 2 mA. To connect the output to the CRT pins, BNC cables were refitted with a save high voltage (SHV) connector on one side while on the other end the BNC connector was kept (fig. 4.2). A 6 kV probe was used to obtain the breakdown voltage, which is around 3 kV caused by the coaxial cable which was not built do sustain high voltages.

1

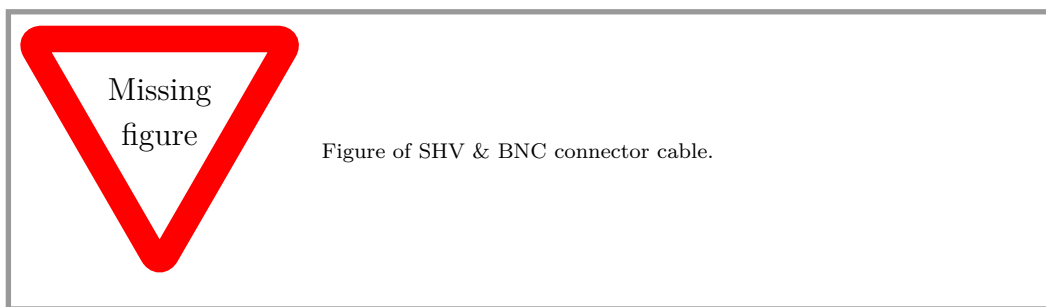
2

3

4

5

6

Somewhere 2.5  
find exact value**Figure 4.2:** Coaxial cable with SHV and BNC connector.

### **4.2.1 Ripple measurement**

Each power supply was measured for its ripple with a set voltage of 2 kV. A 2.5 kV probe (attenuation ratio ) was connected to an oscilloscope set to ac coupling with a timescale of 1 ms. To get the electronic noise of the oscilloscope itself, the probe was shorted and the noise measured. A picture of a measurement is shown in fig. 4.3 with the values summarized in table 4.3. As can be seen, the ripple is very close to the noise level and can not really be distinguished.

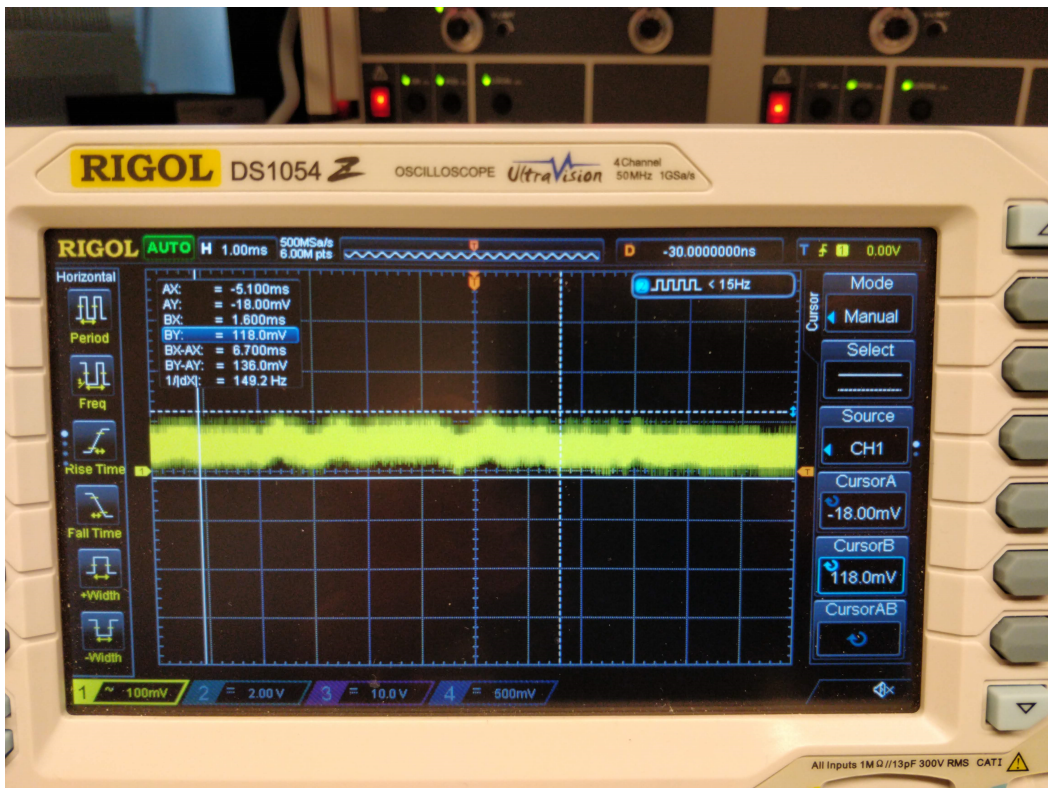


**Figure 4.3:** Measurement of HVPS ripple.

**Table 4.3:** HVPS ripple

device	ripple/mV
short	116
HVPS 1	136
HVPS 2	138
HVPS 3	194
HVPS 4	204

## 4.3 CRT wiring

A schematic of the supplied power is shown in fig. 4.4. A small ac or dc voltage is necessary to drive the heater filament f. This part of the setup is explained in section 4.4.

1  
2  
3  
4

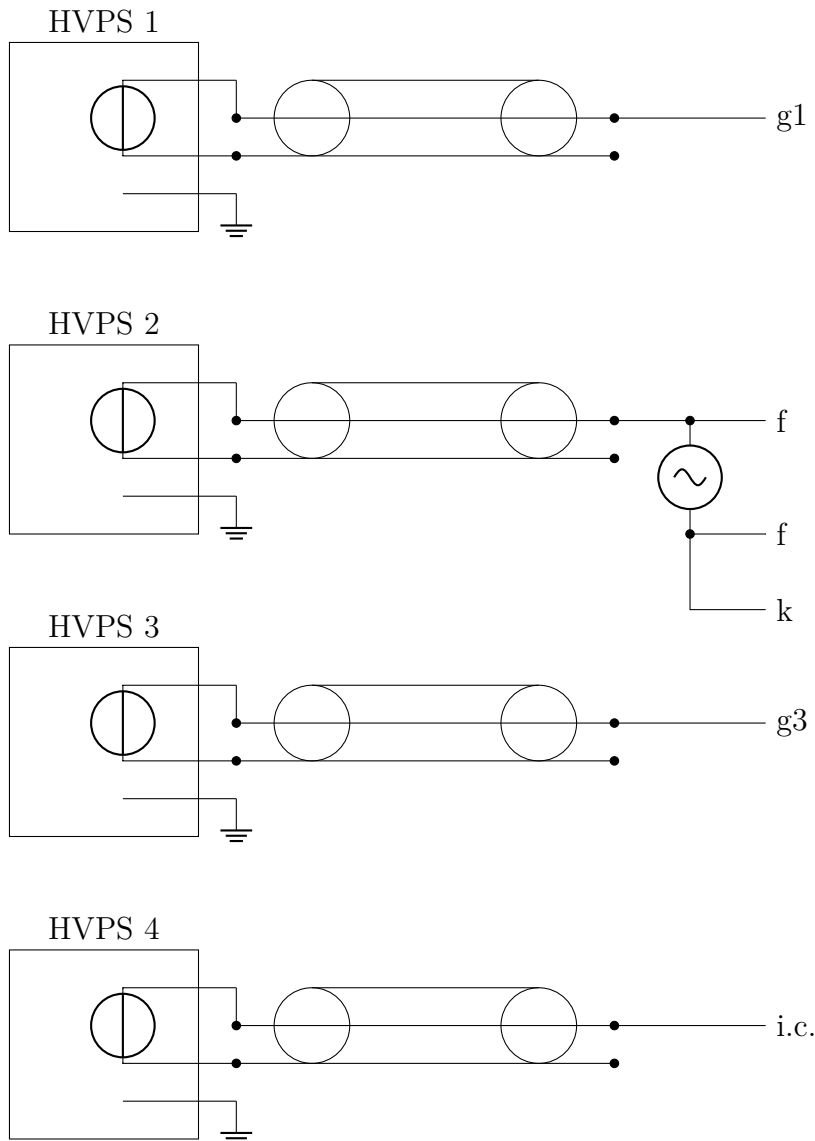


**Figure 4.4:** Schematics of supplying CRT pins with power.

## <sup>1</sup> 4.4 Heater

- <sup>2</sup> The heater provides an adjustable ac voltage, which is used to regulate the temperature  
<sup>3</sup> of the cathode. In the cold state, the heater filament has a an electrical resistitance  
<sup>4</sup> of approximately  $15\ \Omega$ , when the filament is hot, this value rises to  $90\ \Omega$ . The normal  
<sup>5</sup> heater voltage for the D14-363GY/123 during operation is 6.0 V to 6.6 V according to  
<sup>6</sup> [3]. Our ac-power supply (figure 4.5 shows its circuit diagram) consists of an isolation

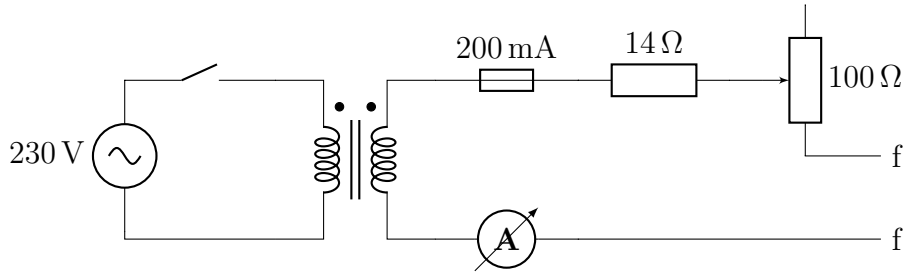


**Figure 4.5:** Circuit diagram of filament power supply.

check if really  $14\Omega$  or if it event exists

transformer (from grid voltage to 12 V), its primary and secondary circuits are isolated up to 4 kV [14]. The power supply has two banana plug sockets to connect to the heater filament. It is connected to the transformer in series with a  $100\Omega$  potentiometer. Using the full resistance, there is a voltage of approximately 5.7 V applied to the heater filament, by lowering the resistance this value can go up to nearly the full voltage of the transformer. The current running through the filament is measured with an integrated amperemeter [15] that measures currents up to two 2 A with mA accuracy.

At the beginning of operation it is recommendable to set the maximum resistance and slowly increase the current to the desired value once the filament is heated up. As the resistance of the cold filament is significantly lower, high onset currents could otherwise damage it.

1  
2  
3  
4  
5  
6  
7  
8  
9  
10  
11

# <sup>1</sup> 5 CRT handling

## <sup>2</sup> 5.1 Opening CRTs

<sup>3</sup> In order to hit the  $^{39}\text{K}$  cloud with an electron beam, it is necessary to cut open the  
<sup>4</sup> CRT. This section explains the different methods which were tried and which resulted  
<sup>5</sup> in clean and easy cuts. All slices were made in a glove box filled with nitrogen gas  
<sup>6</sup> (fig. 5.1) to avoid oxygen poisoning of the cathode.

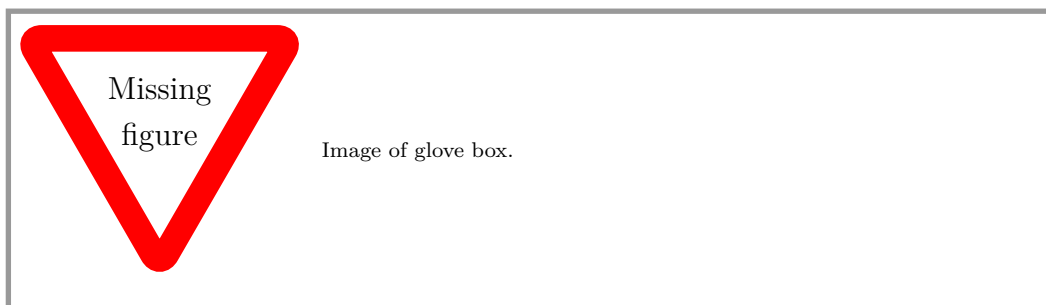


**Figure 5.1:** Glovebox filled with nitrogen gas to open CRTs.

### <sup>7</sup> 5.1.1 Rotary tool

<sup>8</sup> First, a small hole was drilled in the center of the CRT pins to pressurize the CRT  
<sup>9</sup> with nitrogen. Then a diamond wheel attached to a rotary tool was used to cut the  
<sup>10</sup> glass. This method was tried twice, but did not work well, as the method produced a  
<sup>11</sup> lot of glass dust, which adhered to the electron optics. Another obstacle is the plastic  
<sup>12</sup> box, since it is not fully transparent and therefore made more difficult to see inside.

### <sup>13</sup> 5.1.2 Wire cutting

<sup>14</sup> Higher success was achieved by cutting the glass with a heated wire. Two wires were  
<sup>15</sup> put through the glove box, each ending in a ring terminal. A small height adjustable  
<sup>16</sup> stage was built out of optical table parts (fig. 5.2) in which the CRT was put vertically

and looped by an 0.25 mm steel wire (Fe 70/Cr 25/Al 5). It is important to keep a small gap in the loop to avoid an electrical short. Therefore two notches were made in which the wire was fixed.

The assembly was put inside the glove box which was subsequently filled with nitrogen. A current of approximately 2 A to 2.5 A was used to heat the thin wire which resulted in a breaking point inside the CRT glass. This method does not require a CRT pressurization before the cut. In order to not destroy a device by mistake, this procedure can first be tested on drinking glasses.

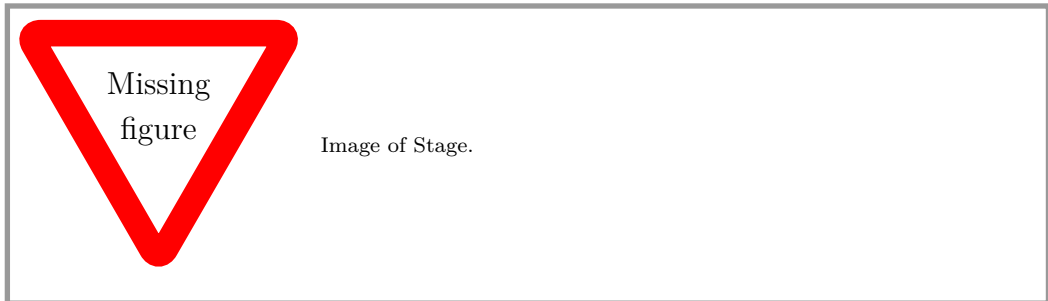


**Figure 5.2:** Stage to cut CRT with wire.

## 5.2 Oxygen poisoning

As mentioned in it is paramount to avoid contact of the cathode with oxygen. Therefore tests with a broken CRT were made to test on how well it can be isolated from air.

The first experiment consisted of filling a drinking glass put upside-down with helium and putting a lighter after a set amount of time. If the fire goes off, it means that oxygen did not get inside. This was tested successfully from 0.5 min to 10 min.

Next, plastic wrap was put on top of the glass filled with nitrogen by a rubber band. The glass was put with the open side up from 3 min to 10 min after which it was turned upside down and the foil was removed. A lighter was put inside and the flame went out again.

To improve the sensitivity, a He leak tester was used. For the first two tests, one plastic foil and one rubber band were used, for the third test three foils and two rubber bands, and for the last test an aluminum foil was hot glued on the CRT to seal it. The measurement locations are shown in fig. 5.3. As shown in table 5.1 using rubber band and clear foil results in the highest leakage while the glue seals much better (glue avg). But care needs to be taken in order ensure that the whole CRT is sealed since even a

## 5 CRT handling

---

- <sup>1</sup> small leak can result in a rate around an order of magnitude above the background  
<sup>2</sup> (glue max).

**Table 5.1:** He leak test.

location	leak rate/(10 <sup>-5</sup> mbar l/s)
1 plastic foil, 1 rubber band	
background	8
plastic foil	20
He gas cylinder	200
1 plastic foil, 1 rubber band	
background	7
plastic foil	20
rubber band	40
3 foils, 2 rubber bands	
background	20
plastic foil	30
rubber band	70
1 aluminum foil, hot glue	
background	6
glue avg	7
glue max	60
aluminum foil	8

## 5 CRT handling

---



(a) plastic foil



(b) rubber band



(c) glue



(d) aluminum

**Figure 5.3:** Measurement locations of He leakage.

# <sup>1</sup> 6 Vacuum test chamber

<sup>2</sup> In order to be able to fit the CRT screen, CF160 flanges were chosen for the test  
<sup>3</sup> chamber. At one point during testing, major changes were made which will be explained  
<sup>4</sup> in section [6.2](#).

## <sup>5</sup> 6.1 First iteration

<sup>6</sup> A 3D render of the chamber is shown in (fig. [6.1](#)). Without a CRT installed, it  
<sup>7</sup> was possible to reach a pressure of  $6.8 \times 10^{-7}$  mbar, while with one the lowest was  
<sup>8</sup>  $2.0 \times 10^{-6}$  mbar.

### <sup>9</sup> 6.1.1 Parts

<sup>10</sup> The center piece consists of a 6-way cross with view ports at the front and bottom.  
<sup>11</sup> A valve was installed at the back in order to flood the chamber with nitrogen when  
<sup>12</sup> installing a new CRT to avoid oxygen poisoning. On the right side, a HiCube 300 Eco  
<sup>13</sup> turbo pump was installed and on the left side a wobble stick was attached with a wire.  
<sup>14</sup> A nipple fitting was installed at the top with a 5 port cluster flange, each being of  
<sup>15</sup> type CF63.

pure nitrogen  
name?

length

<sup>16</sup> In the middle port, a VSH vacuum transducer was installed to measure pressure.  
<sup>17</sup> This needs a 24V dc power supply. On the left, a 19 pin connector was installed to  
<sup>18</sup> supply the necessary voltages to the CRT. Two flanges were equipped with four BNC  
<sup>19</sup> feedthroughs each. One of them was used to connect do the x-, and y-plates, while the  
<sup>20</sup> other connected to the wobble stick and aluminum foil at the CRT screen. Further  
<sup>21</sup> explanation will be given in chapter [8](#). The last port was capped off by a blank flange.

how many pins  
model name?

<sup>22</sup> For the inside wires, stranded copper cables were used. The chamber was sealed by  
<sup>23</sup> rubber gaskets.



**Figure 6.1:** 3D rendering of test chamber.

### 6.1.2 CRT mounting mechanism

Two M8 rods of length   were drilled into the cluster flange. On each, a L-piece was installed between two nuts and they were connected by a hose clamp. Two of these were used to secure the CRT inside the nipple facing the cross (fig. 6.2).

1  
rod length?  
3  
4

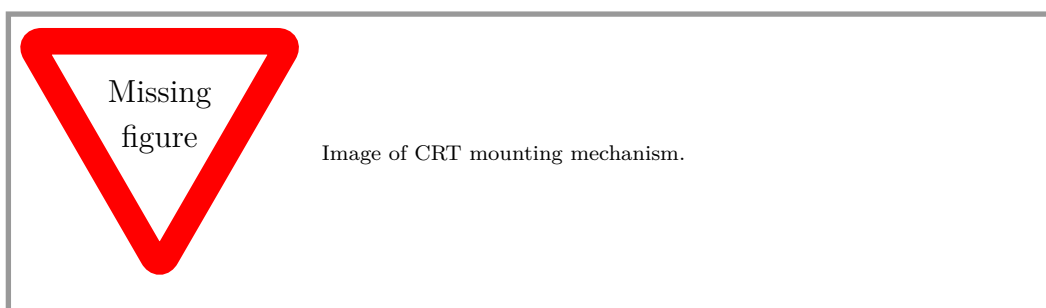


**Figure 6.2:** Image of CRT mounting mechanism.

### <sup>1</sup> 6.1.3 Leak test

<sup>2</sup> Before inserting a CRT, a leak test was performed. First, the chamber was set to a  
<sup>3</sup> pressure of  $10^{-5}$  mbar after which the pump was turned off. The pressure was measured  
<sup>4</sup> once a minute for a duration 3 h. This is shown in fig. 6.3.

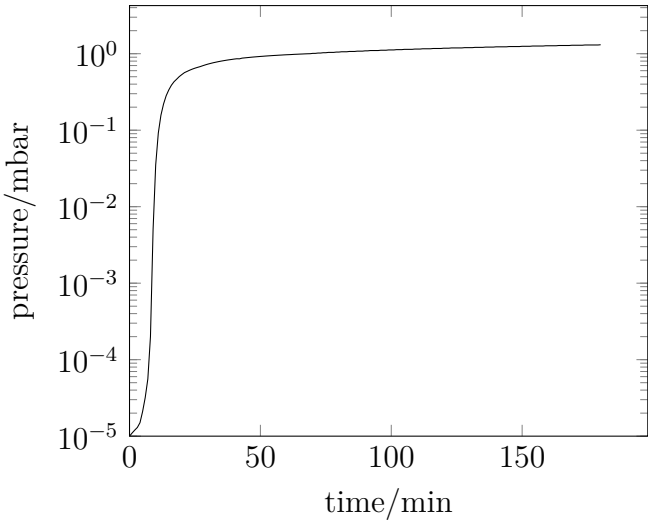


**Figure 6.3:** Leak rate of test chamber after turning off pump.

## <sup>5</sup> 6.2 Second iteration

<sup>6</sup> At one point during experimentation, major changes were made to the chamber. Thanks  
<sup>7</sup> to these, it was possible to reach a pressure of  $1.2 \times 10^{-7}$  mbar.

### <sup>8</sup> 6.2.1 Changes

<sup>9</sup> First, every rubber gasket was changed to a copper one for a better seal, except at the  
<sup>10</sup> cluster flange, since that spot will be opened and closed the most often. Each copper  
<sup>11</sup> stranded cable inside was switched to a coaxial one and the mantle was connected to  
<sup>12</sup> the chamber wall, which was set to ground. A Faraday cup was installed below the  
<sup>13</sup> wobble stick, to accurately measure the beam current (further details in section 8.2).  
<sup>14</sup> The aluminum foil was extended to cover all four sides of the screen.

### 6.2.2 Fastening

When attaching flanges, it is important to start with a low torque and to fasten opposite screws to prevent too much force on one side of the gasket. For M6 screws, the torque was incrementally set to 6 N m, 10 N m, 15 N m and 20 N m and for M8 screws 8 N m, 16 N m and 25 N m. After finishing every opposite screw pair at a set torque, the procedure was repeated twice before going to a higher torque. This was done in order guarantee a tight and even seal.

1  
2  
3  
4  
5  
6  
7

# <sup>1</sup> 7 Deflection Electronics

## <sup>2</sup> 7.1 Demands on the setup

<sup>3</sup> For the QuaK experiment it is paramount to be able to deflect the beam precisely  
<sup>4</sup> and with the right frequency. As previously mentioned, our deflection system simply  
<sup>5</sup> consists of two pairs of parallel plates between which a voltage is applied. Controlling  
<sup>6</sup> this voltage allows us to control the deflection of the beam. Various aspects are  
<sup>7</sup> important here (illustrated in fig. 7.1):

Optional: insert  
Foto of CRT's  
flection plates -  
fig:DeflectionSe

<sup>8</sup> **Offset:** Although the deflection of the beam is controlled by the voltage between the  
<sup>9</sup> plates, it is necessary to be able to set their mean potential as well. During  
<sup>10</sup> normal operation this offset voltage is at 96 V for the x-direction and at 78 V for  
<sup>11</sup> the y-direction.

<sup>12</sup> **Amplitude:** The deflection coefficients in the x and y planes are  $19 \text{ V cm}^{-1}$  and  
<sup>13</sup>  $11.5 \text{ V cm}^{-1}$  respectively (see [3]). We therefore need to be able to supply approx-  
<sup>14</sup> imately 70 V.

<sup>15</sup> **Frequency:** The final goal is to be able to deflect the beam at the hyperfine splitting  
<sup>16</sup> frequency of  ${}^{39}\text{K}$ , which is 461.7 MHz. This is likely to prove impossible with this  
<sup>17</sup> CRT-model, observations at the highest frequency we have tried so far will be  
<sup>18</sup> discussed in section section 8.3.

<sup>19</sup> **Waveform:** Ultimately we want the cold atoms to experience a field that oscillates like  
<sup>20</sup> a sine wave. As a first try it is therefore reasonable to apply a sinusoidal voltage.

<sup>21</sup> **Lissajous curves:** Having the ability to control the deflection in both the x- and the  
<sup>22</sup> y- axis, allows us to have our beam draw out Lissajous Curves (fig. 7.2). By  
<sup>23</sup> applying sine waves of equal frequency to both pairs of deflection plates and by  
<sup>24</sup> being able to control the phase between them we can have the beam oscillate on  
<sup>25</sup> a straight line or a circle. This allows us to generate either a linearly or circularly  
<sup>26</sup> polarized field.

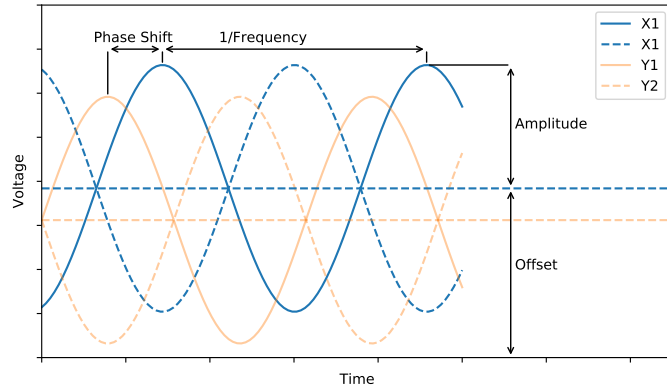


Figure 7.1

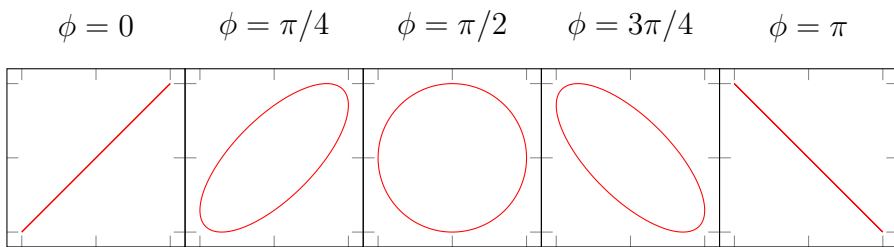


Figure 7.2: Lissajous Curves

## 7.2 Implementation

A first setup with which we can try to obtain the desired voltages is depicted in fig. 7.3. On the very left we have a signal generator that is capable of producing the right frequency (461.7 MHz) this signal is then split up into an x-, and a y-branch. One of the two branches is connected to a phase shifter, which is able to delay the input signal by up to 200°, allowing us to set any desired phase shift between x-, and y-deflection and to correct for inadvertent delays from the other electronics. Both the x-, and y-signal are then amplified using (amplifier) . In the final step, a center tapped transformer allows us to produce voltages for the plates X1 and X2 (or Y1 and Y2 respectively) with a phase shift of exactly 180° between them. By setting the center tap to the desired offset potential, we should get the voltage curves described above. To understand this setup in more detail, it is useful to examine its most important parts more closely:

**Amplifier:** Up to now we have used the XXX and the YYY amplifier, they amplify the signal by a fixed gain of (How much?) , inputs and outputs can simply be

1  
2  
3  
4  
5  
6  
7  
Find out which  
10  
11  
12  
13

14 which model?  
15 which model?  
Check amplifier  
specifications

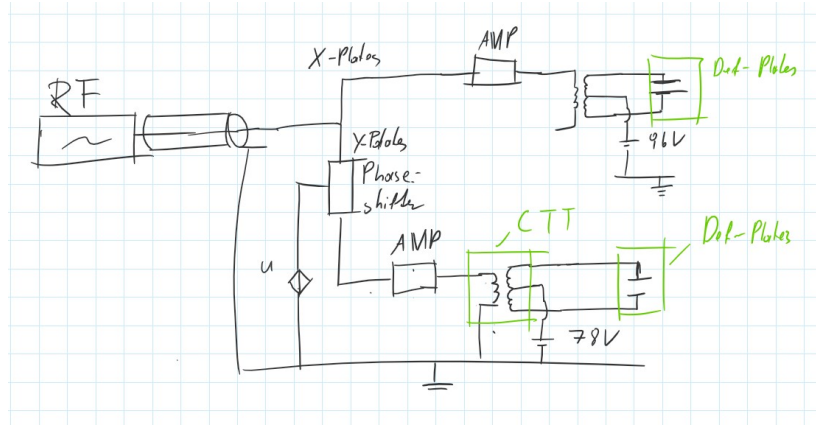


Figure 7.3: Deflection circuit

1 connected via BNC cables, the amplifier is powered by a linear power supply  
 2 with a DC voltage of 24 V via two banana plugs in the front. Since we want to  
 3 control the Lissajous curves shapes (as the deflection coefficients for the x- and  
 4 y- plates differ), it is desirable to be able to adjust the amplifier gain in future  
 5 versions of the setup.

6 **Center Tapped Transformer:** The center tapped transformer we use is the Mini-  
 7 Circuits TC8-1G2+ ([16]), a transformer for frequencies between 2 MHz to  
 8 500 MHz, with an impedance ratio of 8. Figure 7.6 shows how the center tapped  
 9 transformer is implemented. The in- and outputs, as well as the bias voltage  
 10 can be connected via BNC cables. As usual, the shields of all these cables are  
 11 connected to ground, furthermore they are connected to each other and to the  
 12 housing. As a safety feature, both outputs X1 and X2 are directly connected  
 13 to the bias through an arrangement of diodes: Two connections, each with a  
 14 normal diode and a Zener diode facing in opposite directions. The breakthrough  
 15 voltage of the Zener diode is 200 V, during normal operation the voltage on it  
 16 stays below this value and none of the connections let any current through as  
 17 one of the two diodes is always blocking it. However if one of the plates in the  
 18 CRT accidentally comes in contact with high voltage, the connection with the  
 19 appropriately oriented Zener diode opens up, preventing a voltage spike on the  
 20 center tapped transformer and thereby protecting the electronics connected to  
 21 its primary circuit. At the point of writing there are still some problems with  
 22 the behavior of the center tapped transformer, the capacitance of the diodes  
 23 introduces an undesired phase shift between the two signals. Figure 7.5a shows  
 24 the circuit's behavior at 465 MHz without its diodes, here the signals are shifted  
 25 by  $120 \text{ ps} \cong 20^\circ = 0.35 \text{ rad}$ . Additionally, applying a bias voltage leads to differing  
 26 amplitudes, as can be seen in fig. 7.5b.

Optional: Go to lab and measure their performance with an Oszi.

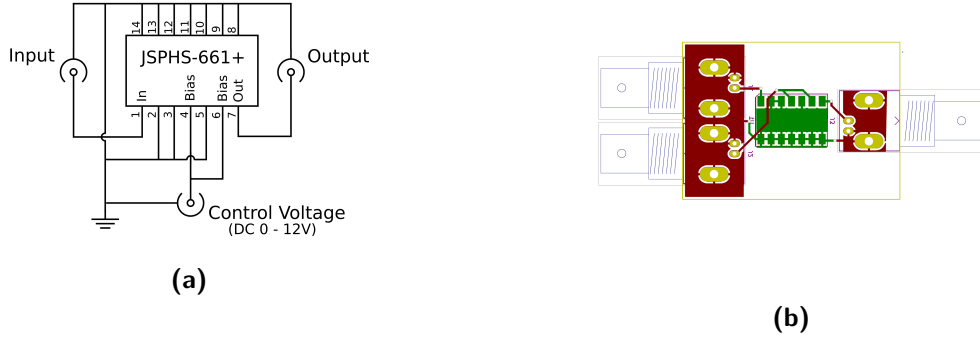
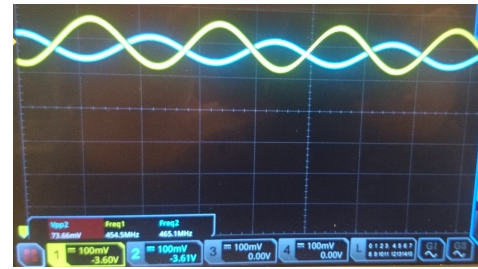


Figure 7.4



(a) Signal of center tapped transformer without diodes, unbiased at 465 MHz



(b) Signal of center tapped transformer without diodes, biased at 465 MHz

Figure 7.5

**Phase Shifter:** To control the phase shift between the x- and y-deflection plates, we use a Mini-Circuits [17] phase shifter. This part was put in a housing ([18]) on a separate PCB and can be connected via BNC cables. Figure 7.4a shows how the phase shifter is connected and fig. 7.4b shows the corresponding PCB layout. Note that again the shields of the BNC cables are connected among each other and to the housing. The JSPHS-661+ is designed for frequencies in the range 400 MHz to 600 MHz. By applying a DC voltage of 0V to 12V to the bias connector, it is possible to introduce a phase shift of up to 200° to the signal.

(figure) \_\_\_\_\_  
 (Performance) \_\_\_\_\_

1  
2  
3  
4  
5  
6  
7  
8

Insert fotos of finished circuits in 10 housings

Optional: Go to the Lab, set up the whole thing and look at its performance on the oscilloscope

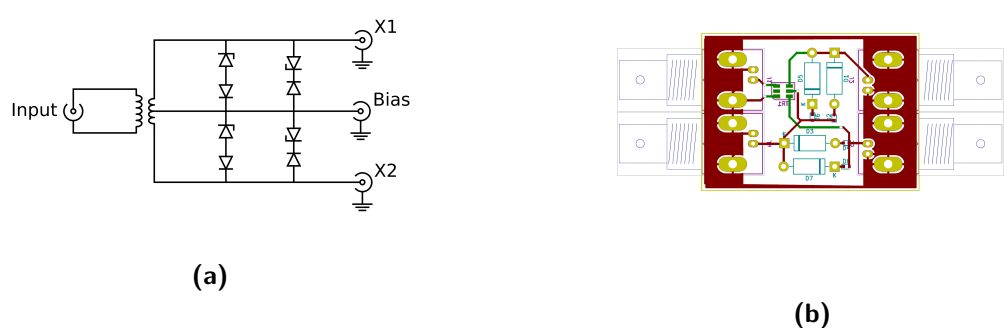


**Figure 7.6**

# 8 Beam Characterization

## 8.1 Aluminum foil

In fig. 8.1 the inside of the 6-way cross of the first iteration is shown. On one side of the phosphor screen, aluminum foil was attached to simulate the aquadag coating inside a CRT. The beam was deflected on the aluminum foil and the BNC output was connected to ground through an ammeter to measure the beam current. As shown in fig. 8.2 there is close to no difference in the filament voltage (and therefore heating power) between an opened and sealed CRT while the beam current on the aluminum foil varies widely. One possible reason could be that electrons scatter around and not all choose the wire path to ground. Therefore a Faraday cup (see section 8.2) was used in the second iteration.

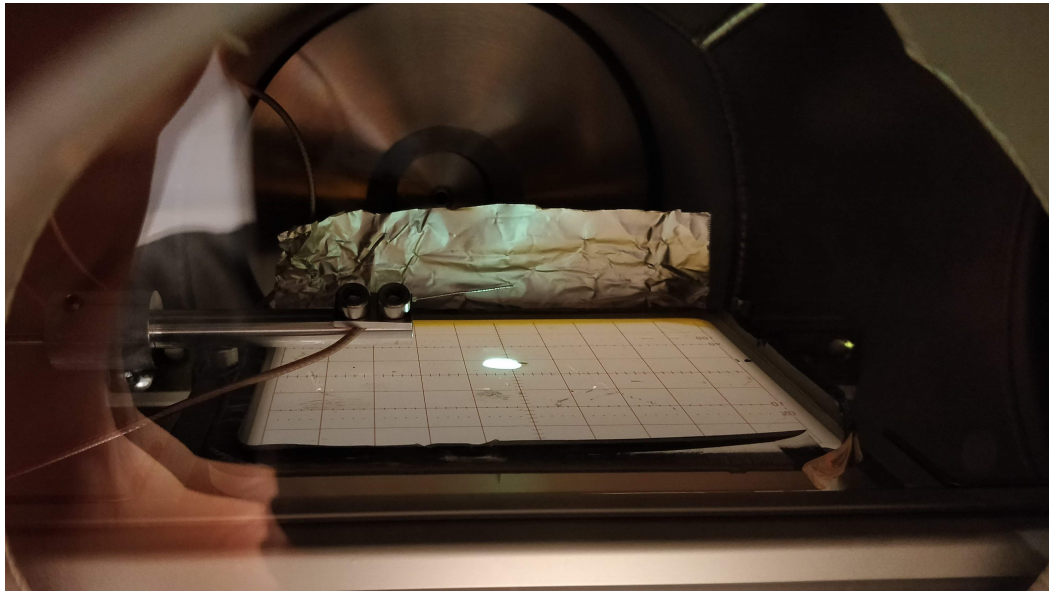


**Figure 8.1:** Front view of vacuum chamber (first iteration).

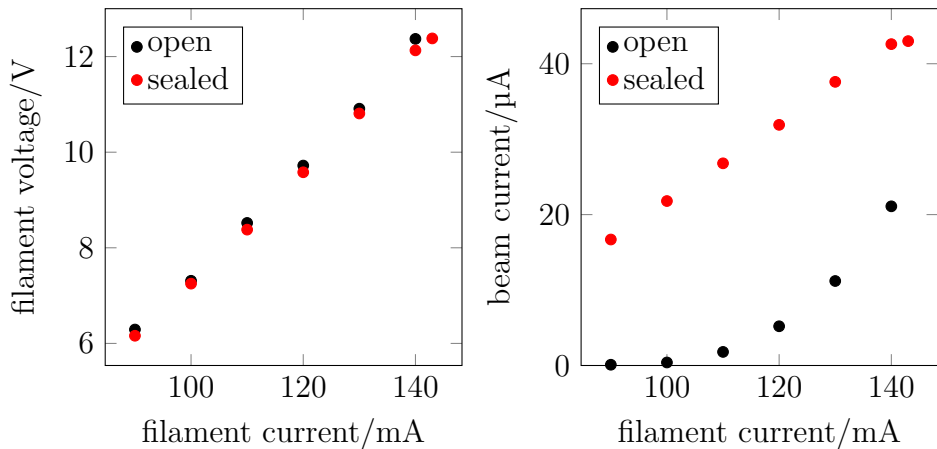


**Figure 8.2:** Difference in filament voltage and beam current between an open and sealed CRT.

## 1 8.2 Faraday cup

2 In order to accurately measure the beam current, a Faraday cup was built. A schematic  
 3 is shown in fig. 8.3. A copper tube was cut at an  $45^\circ$  angle on one side and a Cu-sheet  
 4 was soldered at the top and bottom. A small hole of around 5 mm was drilled at  
 5 the top and a coaxial cable was attached on the mantle which connects to a BNC  
 6 feedthrough at the top of the chamber. The small opening and bent floor were made  
 7 in order to reduce backscattering as indicated by blue arrows. At the top surface a  
 8 phosphor coating was applied in order to make the beam visible which made it easier  
 9 to guide it into the opening hole.

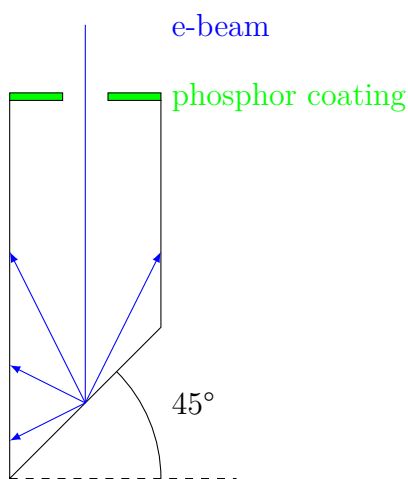


**Figure 8.3:** Schematics of Faraday cup.

With this improved setup, the beam current was measured again. A summary is shown in fig. 8.4. It can be seen that a current of over  $300 \mu\text{A}$  was achieved, which is more than the necessary amount for the experiment. A problem is the fact, that the current is not stable. A measurement on the next day under the same settings resulted in a current between  $50 \mu\text{A}$  to  $120 \mu\text{A}$ .

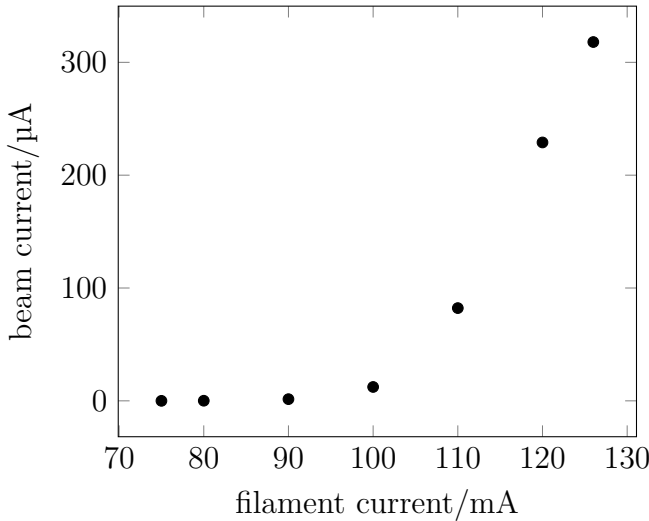


**Figure 8.4:** Beam current dependence on heater current.

### 8.3 Deflection frequency

This section describes a few observations that were made when letting the electron beam interact with a short piece of wire, that is mounted to the wobble stick. Originally, we hoped to be able to measure the beam waist, using the knives edge method, i.e. observing the current transported by the beam, while slowly moving a razor blade into the beam path. However the beam is bent, when it passes closely to a conductive part. Whenever we moved our wire close to the beam, the visible spot on the Phosphorous screen below was distorted. This will probably complicate the measurement of the beam waist in the future. When the wire is connected to an oscilloscope, one can see a sharp increase in voltage, when it is moved into the beam. This can be used to see whether our deflection plates work properly and to test how fast we are able to deflect the beam. If the beam oscillates back and forth on a straight line and crosses the wire on the midway point, we should see a spike in voltage on the wire, which repeats with twice the frequency of the beam. If the wire is not on the midway point, the periods between consecutive spikes should sum up to the period of the beam's oscillation (see fig. 8.5). At low frequencies we have indeed observed this behavior.

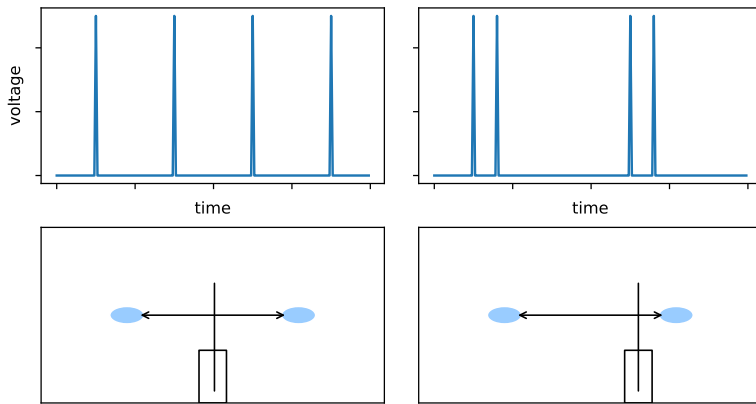


**Figure 8.5**

<sup>1</sup> As the frequency is increased, the magnitude of the signal decreases. This is easily  
<sup>2</sup> explained by the fact that the remain time close to the wire is inversely proportional  
<sup>3</sup> to the frequency and the amplitude of beams deflection. It was possible to see the  
<sup>4</sup> spikes up to a frequency of 100 kHz, before they were obscured by noise and some  
<sup>5</sup> other periodical, but so far unexplained artifacts. At high deflection frequencies, the  
<sup>6</sup> wire may also pick up some signal form the capacitive charging and discharging of the  
<sup>7</sup> deflection plates and the corresponding oscillating electromagnetic field. In order to be  
<sup>8</sup> able to see what happens at higher frequencies, a higher beam current and a smaller  
<sup>9</sup> deflection amplitude would be beneficial, however the most important factor in order  
<sup>10</sup> to understand what is happening is better focus and a better beam shape.

# 9 Next Steps

To conclude this report, we will point out some of the next steps that need to be taken in order to advance the electron beam setup.

**Beam current stability:** The most important challenge at this moment is the ability to produce a reproducible, stable, and sufficiently strong beam. In order to achieve this, more research on cathodes and their susceptibility to oxygen poisoning needs to be conducted. It may also prove useful to add another high voltage power supply to the setup in order to tune the filament potential independently from the Wehnelt cylinder.

**Spot size characterisation:** As previously mentioned, our original attempt was, to probe the electron beam's profile using a thin piece of wire on the wobble stick. However, we have observed that the beam got warped when passing close to conductive materials, therefore a different approach is needed.

**Heating mechanism:** As high currents will degrade the filament and cathode, it is desirable to be able to tune the heater current down to 0 mA continuously. Such a power supply needs to support a bias voltage of around  $-2\text{ kV}$ .

**Lissajous Curves:** Regarding the deflection electronics, the first issue that needs to be addressed is the fact that it is not possible to produce a clean sine wave when a bias voltage is applied to the center tapped transformer. Furthermore, it is recommended to implement the over voltage protection described previously with very low capacitance diodes. In the future, the setup should be able to produce Lissajous curves at the  $^{39}\text{K}$  hyperfine transition frequency of 461.7 MHz.

1

2

3

4

5

6

7

8

9

10

11

12

13

14

15

16

17

18

19

20

21

2 Check whether have explained benchmarks for beam (waist, current, frequency)

# <sup>1</sup> Todo list

<sup>2</sup>	■ set date to English . . . . .	A
<sup>3</sup>	■ können die Maße stimmen? . . . . .	4
<sup>4</sup>	Figure: Image of CRT . . . . .	6
<sup>5</sup>	■ namechange? . . . . .	11
<sup>6</sup>	■ <a href="http://www.tobiastiecke.nl/archive/PotassiumProperties.pdf">http://www.tobiastiecke.nl/archive/PotassiumProperties.pdf</a> . . . . .	13
<sup>7</sup>	■ 1:100 or 100:1 . . . . .	13
<sup>8</sup>	■ somewhere 2.5-4, find exact value . . . . .	14
<sup>9</sup>	Figure: Figure of SHV & BNC connector cable. . . . .	14
<sup>10</sup>	■ 100:1 or 1:100 . . . . .	15
<sup>11</sup>	■ check if really $14\Omega$ or if it event exists . . . . .	18
<sup>12</sup>	Figure: Image of glove box. . . . .	19
<sup>13</sup>	Figure: Image of Stage. . . . .	20
<sup>14</sup>	■ pure nitrogen name? . . . . .	23
<sup>15</sup>	■ length . . . . .	23
<sup>16</sup>	■ how many pins and model name? . . . . .	23
<sup>17</sup>	■ rod length? . . . . .	24
<sup>18</sup>	Figure: Image of CRT mounting mechanism. . . . .	24
<sup>19</sup>	■ Optional: insert Foto of CRT's deflection plates - fig:DeflectionSetup . . . . .	27
<sup>20</sup>	■ Find out which amplifier . . . . .	28
<sup>21</sup>	■ which model? . . . . .	28
<sup>22</sup>	■ which model? . . . . .	28
<sup>23</sup>	■ Check amplifier specifications . . . . .	28
<sup>24</sup>	■ Optional: Go to the lab and measure their performance with an Oszi. . . . .	29

## 9 Next Steps

---

■ Insert fotos of finished circuits in housings . . . . .	30	1
■ Optional: Go back to the Lab, set up the whole thing and look at its performance on the oszi . . . . .	30	2
■ Check whether we have explained the benchmarks for the beam (waist, current, frequency) . . . . .	36	3
	4	4
	5	5

# References

- [1] Tobias Tiecke. *Properties of Potassium*. URL: <https://tobiastiecke.nl/archive/PotassiumProperties.pdf> (visited on 05/15/2020).
- [2] Wolfgang Demtröder. *Experimentalphysik 3*. Springer-Lehrbuch. Berlin, Heidelberg: Springer-Verlag Berlin Heidelberg, 2009. Chap. 2.6.1.
- [3] Frank Philipse. *D14363GY123*. URL: <https://frank.pocnet.net/sheets/186/d/D14363GY123.pdf> (visited on 03/10/2020).
- [4] Jerry C. Whitaker and Fla. [Verlag] CRC Press Boca Raton. *Power vacuum tubes handbook*. Third edition. Electronics handbook series. Boca Raton, FL: CRC Press.
- [5] Chuck deVere. *Cathode-Ray Tubes*. 1969.
- [6] Aviv Keshet and Wolfgang Ketterle. “A Distributed, GUI-based, Computer Control System for Atomic Physics Experiments”. In: *Review of Scientific Instruments* 84.1 (2013), p. 015105.
- [7] Aviv Keshet. *The Cicero Word Generator*. URL: <https://github.com/akeshet/Cicero-Word-Generator> (visited on 02/20/2020).
- [8] Aviv Keshet. *Cicero Word Generator Technical and User Manual*. URL: <http://akeshet.github.io/Cicero-Word-Generator/Cicero%20Technical%20and%20User%20Manual.pdf> (visited on 02/24/2020).
- [9] Microsoft. *Download .NET (Linux, macOS, and Windows)*. URL: <https://dotnet.microsoft.com/download> (visited on 02/24/2020).
- [10] National Instruments. *NI Driver Downloads - National Instruments*. URL: <https://www.ni.com/en-us/support/downloads/drivers.html> (visited on 02/24/2020).
- [11] National Instruments. *NI Software Gives C++ Runtime Error “Terminated in an Unusual Way” - National Instruments*. URL: <https://knowledge.ni.com/KnowledgeArticleDetails?id=kA00Z0000019YOnSAM&l=en-US> (visited on 02/24/2020).
- [12] Rohde & Schwarz. *HM 507*. URL: [https://cdn.rohde-schwarz.com/hameg-archive/HM507\\_english.pdf](https://cdn.rohde-schwarz.com/hameg-archive/HM507_english.pdf) (visited on 03/28/2020).
- [13] FuG Elektronik GmbH. *HVPS Series HCP*. URL: [https://www.fug-elektronik.de/wp-content/uploads/pdf/Datasheets/EN/HCP\\_data\\_sheet.pdf](https://www.fug-elektronik.de/wp-content/uploads/pdf/Datasheets/EN/HCP_data_sheet.pdf) (visited on 03/23/2020).
- [14] Myrra SAS. *Data Sheet 44231*. URL: <http://www.farnell.com/datasheets/92205.pdf> (visited on 04/07/2020).

## References

---

- [15] Murata Power Solutions. *ACA-20PC manual*. URL: <https://www.murata.com/products/productdata/8807023804446/aca20pc.pdf> (visited on 04/07/2020).1  
2
- [16] Mini-Circuits. *TC8-1G2+*. URL: <https://www.minicircuits.com/pdfs/TC8-1G2+.pdf> (visited on 05/05/2020).3  
4
- [17] Mini-Circuits. *JSPHS-661+ Data Sheet*. URL: <https://www.minicircuits.com/pdfs/JSPHS-661+.pdf> (visited on 05/05/2020).5  
6
- [18] Hammond Manufacturing. *1455D601RD*. URL: <https://www.hammfg.com/files/parts/pdf/1455D801RD.pdf> (visited on 05/05/2020).538  
539